

Laser-induced fluorescence excitation spectroscopy of N_2^+ produced by VUV photoionization of N_2 and N_2O

Masakazu Mizutani,^a Hiromichi Niikura,^b Atsunari Hiraya^c and Koichiro Mitsuke^{a*}

^aDepartment of Vacuum UV Photoscience, Institute for Molecular Science, Myodaiji, Okazaki 444-8585, Japan, ^bThe Graduate University for Advanced Studies, Institute for Molecular Science, Myodaiji, Okazaki 444-8585, Japan, and ^cFaculty of Science, Hiroshima University, Kagamiyama, Higashi-Hiroshima 739, Japan. E-mail: mitsuke@ims.ac.jp

(Received 4 August 1997; accepted 3 November 1997)

Synchrotron radiation emitted from the UVSOR storage ring is monochromated by a grazing-incidence monochromator and introduced coaxially with the second harmonic of a mode-locked Ti:sapphire laser. Sample gases, N_2 and N_2O , are photoionized into vibronically ground N_2^+ with the fundamental light of the undulator radiation at 18.0 and 18.6 eV, respectively. Laser-induced fluorescence (LIF) excitation spectra of N_2^+ from N_2 and N_2O are measured in the laser wavelength region of the ($B^2\Sigma_u^+$, $v' = 0$) \leftarrow ($X^2\Sigma_g^+$, $v'' = 0$) transition at 389–392 nm. The LIF excitation spectra of N_2^+ exhibit two maxima due to the *P* and *R* branches in which rotational bands are heavily overlapped. The rotational temperature is determined by simulating an LIF excitation spectrum by using the theoretical intensity distribution of rotation bands convoluted with the spectral width of the laser.

Keywords: synchrotron radiation–laser combinations; pump–probe experiments; laser-induced fluorescence; N_2^+ ; rotational distributions.

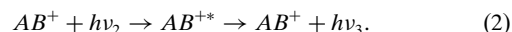
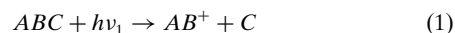
1. Introduction

There is a growing interest in combining synchrotron radiation with the laser, since high-resolution or ultra-fast lasers are expected to open a new field for studies on the dynamical behaviour of excited molecules in the VUV or soft X-ray region. Nevertheless, only a few attempts have been made at pump–probe experiments of molecules using synchrotron radiation and a laser: photoelectron spectroscopy of atomic iodine produced from I_2 (Nahon *et al.*, 1990, 1991), photoelectron spectroscopy of N_2 and HCN produced from *s*-tetrazine (Nahon *et al.*, 1992), and photoionization of atomic iodine produced from CH_3I (Mizutani *et al.*, 1997). In all of these cases a laser is used as a photolysis source which leads to dissociation of molecules.

To take maximum advantage of the features of the laser, *i.e.* its excellent spectral and temporal resolution, we should examine the feasibility of the laser in detecting and analysing products resulting from VUV or soft X-ray photoexcitation. Two kinds of products may be taken into account: ions and neutral molecules. Probing ionic fragments by a laser with high resolving power provides their precise internal distribution. This allows us to discuss the mechanism of dissociative ionization preceded by direct ionization or autoionization, on the basis of the detailed

character of a relevant ionic potential energy surface. Furthermore, decay dynamics of vibronically excited ions, which is still an open question, can be studied by laser spectroscopy of ground-state ions prepared by VUV photoexcitation (*e.g.* single vibronic level dispersed fluorescence spectroscopy). On the other hand, the internal distribution of neutral fragments produced *via* superexcitation usually contains information on predissociation dynamics of superexcited states. The quantum yield for formation of a pair of non-radiative neutral fragments from a superexcited state is frequently comparable with or higher than that for its autoionization (Hikosaka *et al.*, 1997). Such dark species can only be observed by means of pump–probe experiments combining synchrotron radiation and a laser.

A pump–probe experiment combining synchrotron radiation and a laser quite differs from that using two lasers operating synchronously at a lower repetition rate (1–100 Hz). Most of the difficulties in performing the former type of experiments arise essentially from the temporal structure of synchrotron radiation pulses characterized by a frequency of $\sim 10^8$ Hz. The count rate of the probe signal is determined by a time-averaged number density of photolysis products, whether synchrotron radiation is adopted as a pump or probe light. The average number density is extremely low, owing to a short average residence time (10^{-6} – 10^{-7} s) of an ion or excited molecule in a probing region. Let us take an example of a typical pump–probe experiment for a triatomic molecule *ABC* in the gas phase,



The fragment AB^+ is produced by photolysis light ($h\nu_1$) in process (1), and detected by laser-induced fluorescence (LIF) excitation spectroscopy in process (2). When a 10 Hz dye laser is used as a probe light ($h\nu_2$), the signal count rate of the fluorescence ($h\nu_3$) is expected to be 11–12 orders of magnitude lower by selecting monochromated synchrotron radiation from a bending magnet ($\sim 1 \times 10^{10}$ photons s^{-1}) as $h\nu_1$, than by selecting a 10 Hz 10 mW excimer laser synchronized with the dye laser.

In order to overcome the low count rate, synchrotron radiation and a laser are combined in the present study at a beamline from an undulator, which provides two or three orders of magnitude higher photon flux than a bending magnet. In addition, we choose the second harmonic of a Ti:sapphire laser. Its wide tunability in the UV–visible region contributes towards our wide selection of target molecules and their vibronic states. As the most appropriate starting point, we try to observe LIF signals of N_2^+ ions which are produced from N_2 or N_2O by VUV excitation with synchrotron radiation. As far as we know, this is the first report of gas-phase LIF excitation spectroscopy of products prepared by photoionization with synchrotron radiation.

2. Experimental methods

Fig. 1 shows a schematic arrangement of the apparatus for synchrotron radiation–laser combination experiments. A sample gas of N_2 or N_2O is expanded from a nozzle made of a multi-channel capillary array plate into a photoionization vacuum chamber. The molecular beam intersects at 90° with the monochromated undulator light supplied from beamline BL3A2 of the UVSOR storage ring in Okazaki. The size of the photon beam is $\sim 1 \times 1$ mm in the intersection region. Only $N_2^+(X^2\Sigma_g^+, A^2\Pi_u)$

ions are produced, because the undulator photon energy, E_{SR} , is set below the ionization threshold for formation of $N_2^+(B^2\Sigma_u^+, v' = 0)$ from N_2 or N_2O . The second harmonic of a mode-locked Ti:sapphire laser, which is introduced so as to counterpropagate the undulator light, probes $N_2^+(X^2\Sigma_g^+, v_i'' = 0)$ ions by means of LIF excitation spectroscopy. The laser wavelength is scanned in the region of the 0–0 band, *i.e.* the $(B^2\Sigma_u^+, v' = 0) \leftarrow (X^2\Sigma_g^+, v_i'' = 0)$ transition at 389–392 nm. The fluorescence is monitored at 427 ± 4 nm, which corresponds to the $(B^2\Sigma_u^+, v' = 0) \rightarrow (X^2\Sigma_g^+, v_f'' = 1)$ transition. The fluorescence is collected with an input optics perpendicularly to the photon and molecular beams, dispersed by a monochromator (Ritsu, MC-10N), and detected by a photomultiplier (Hamamatsu, R464S). A colour filter glass is frequently placed in front of the monochromator to eliminate the scattering laser light. The ambient pressure in a vacuum chamber is monitored by an ionization gauge and kept constant at 3×10^{-5} torr, when the neat sample of N_2 or N_2O is introduced. The effect of collisions can therefore be neglected in the intersection region. Commercial high-purity gases are used without further purification (N_2 , Nihon Sanso, 99.995% pure; N_2O , Showa Denkou, 99.99% pure).

The output of the photomultiplier is processed by a pre-amplifier and a constant fraction discriminator, and fed into the input of a dual-channel gated photon counter (Stanford Research Systems, SR400). An optical chopper (Stanford Research Systems, SR540) modulating the laser beam with a 50% duty ratio is used to alternate the data-acquisition cycle of the laser on and off at 400 Hz in combination with the photon counter. Thereby, we are able to compensate the transient changes or long-term drifts in the experimental conditions, such as a monotonic decrease in the synchrotron radiation photon flux and the variation of the sample pressure.

Details of the undulator radiation and laser system are described elsewhere (Mizutani *et al.*, 1997). The fundamental light of the undulator radiation is reflected by a prefocusing mirror and introduced through an entrance slit into a constant-deviation grazing-incidence-type monochromator with a 2.2 m focal length (Ishiguro *et al.*, 1989). The monochromated light is focused by a postfocusing mirror onto the intersection region. When both the entrance and exit slits of the monochromator are 200 μm wide, a typical photon intensity is 7.8×10^{14} photons

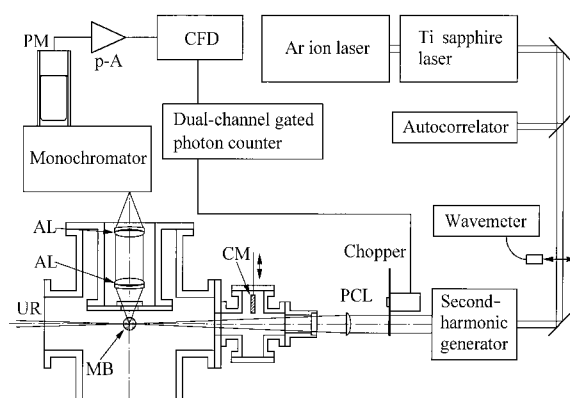


Figure 1

Schematic arrangement of the apparatus for synchrotron radiation–laser combination experiments. PM, photomultiplier; p-A, pre-amplifier; CFD, constant fraction discriminator; AL, spherical achromatic lenses; UR, monochromated undulator radiation; MB, cross section of a molecular beam expanded from a nozzle; CM, gold-mesh current monitor; PCL, spherical plano-convex lens.

$s^{-1} \text{cm}^{-2}$. In this condition the spectral resolution is estimated to be 30 meV (FWHM). The temporal profile of the undulator pulse is represented by a Gaussian function with a FWHM of approximately 400 ps.

A Ti:sapphire laser (Spectra Physics Lasers, Tsunami, 3950-L2S) is pumped by a 9–9.5 W Ar ion laser operated on all lines. The pulse duration, τ_F , of the fundamental (~ 780 nm) is determined by means of a scanning autocorrelator to be ~ 1.8 ps. The second harmonic is generated by using a lithium triborate (LBO) crystal (Spectra Physics Lasers, frequency doubler, 3980-1S) and its wavelength can be changed between 365 and 420 nm. The second harmonic is separated with dichroic mirrors and focused using a fused silica spherical plano-convex lens (focal length ~ 500 mm) onto the intersection region. Typical output powers of the laser are 1.1 and 100 mW for the fundamental (780 nm) and the second harmonic (390 nm), respectively. The pulse energy of the second harmonic is 1.1 nJ (2.2×10^9 photons pulse $^{-1}$) at 389–392 nm. The pulse duration and the spectral resolution of the second harmonic are estimated theoretically (Nebel & Beigang, 1991) from τ_F to be 1.2 ps and 9.2 cm^{-1} , respectively, if we assume a sech^2 pulse shape and Fourier-transform-limit conditions. Thus, only 0.65% of the laser photon flux is available for excitation of a rotational level of $N_2^+(X^2\Sigma_g^+, v_i'' = 0)$ because of a narrow Doppler width (0.06 cm^{-1}), so that the effective laser intensity is evaluated to be 1.3×10^{17} photons $s^{-1} \text{cm}^{-2}$. The Ti:sapphire laser can operate synchronously with a master oscillator (90.115 MHz) for a main RF cavity on the UVSOR storage

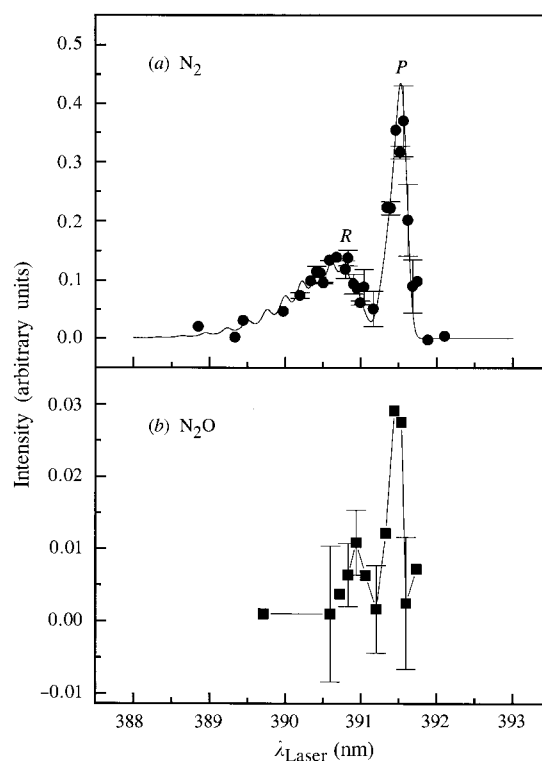


Figure 2

Laser-induced fluorescence excitation spectra of the $(B^2\Sigma_u^+, v' = 0) \leftarrow (X^2\Sigma_g^+, v_i'' = 0)$ transition of N_2^+ which is prepared (a) by photoionization of N_2 at $E_{SR} = 18.0$ eV and (b) by that of N_2O at $E_{SR} = 18.6$ eV. The monitored fluorescence at 427 ± 4 nm is ascribed to the $(B^2\Sigma_u^+, v' = 0) \rightarrow (X^2\Sigma_g^+, v_f'' = 1)$ transition. The solid line in (a) represents a spectrum at $T = 300$ K calculated by using the theoretical intensity distribution of rotation bands [equations (3)–(5)] convoluted with the laser spectral width of 9.2 cm^{-1} . The dashed line in (b) is to guide the reader's eye.

ring; in the present study the definite synchronization is unnecessary because the interval time of the synchrotron radiation pulse (11.097 ns) is considerably shorter than the average residence time (2.1×10^{-6} s) of the primarily produced $N_2^+(X^2\Sigma_g^+)$.

3. Results and discussion

Fig. 2 shows LIF excitation spectra of the $(B^2\Sigma_u^+, v' = 0) \leftarrow (X^2\Sigma_g^+, v_i'' = 0)$ transition of N_2^+ which is prepared either by photoionization of N_2 at $E_{SR} = 18.0$ eV (Fig. 2a) or by that of N_2O at $E_{SR} = 18.6$ eV (Fig. 2b). Data points are obtained from the difference between the fluorescence signal counts with and without the laser as a function of the laser wavelength. In Fig. 2(b), E_{SR} of 18.6 eV is almost equal to the resonance energies of the $3d\pi$ and $4s\sigma$ states converging to $N_2O^+(C^2\Sigma^+)$ (Shaw *et al.*, 1992). Hence, most N_2^+ ions are considered to be produced by autoionization of these Rydberg states. We have tried to observe an LIF excitation spectrum at 388.5 nm of the $(B^2\Sigma_u^+, v' = 1) \leftarrow (X^2\Sigma_g^+, v_i'' = 1)$ transition of N_2^+ from N_2 or N_2O , but the reproducibility is poor owing to low count rates.

The spectral features of Figs. 2(a) and 2(b) can be understood in terms of the P and R branches arising from primary rotational distributions of $N_2^+(X^2\Sigma_g^+, v_i'' = 0)$. Rotational structures would be partially resolved because $B' + B'' = 4$ cm^{-1} is half as large as the theoretical spectral resolution, 9.2 cm^{-1} , of the laser, where B' and B'' represent the rotational constants of the $(B^2\Sigma_u^+, v' = 0)$ and $(X^2\Sigma_g^+, v_i'' = 0)$ states, respectively. In practice, rotational levels are indiscernible, probably due to a much worse experimental resolution (~ 15 cm^{-1}). A band-head lies in the P branch, since the relation $B' > B''$ holds. The fluorescence count rate at 390.61 nm, around which the envelope of the R branch makes a peak, is 2.1 counts s^{-1} for N_2^+ produced from N_2 . This count rate agrees well with that obtained theoretically by an order-estimation procedure. Details of this comparison will be described in a forthcoming paper.

The rotational temperature, T , of $N_2^+(X^2\Sigma_g^+, v_i'' = 0)$ produced from N_2 can be evaluated by simulating the experimental points in Fig. 2(a). We calculate the theoretical intensity distribution of rotation bands (Herzberg, 1966)

$$I(N'') \propto (N' + N'' + 1) \xi(N'') \exp[-B''N''(N'' + 1)/kT] \quad (3)$$

convoluted with the laser spectral width of 9.2 cm^{-1} (FWHM) at transition frequencies,

$$\nu = \nu_{00} + (B' + B'')(N'' + 1) + (B' - B'')(N'' + 1)^2 \quad (4)$$

for the R branch, and

$$\nu = \nu_{00} - (B' + B'')N'' + (B' - B'')N''^2 \quad (5)$$

for the P branch. In these expressions, N' and N'' denote the rotational quantum numbers of the $(B^2\Sigma_u^+, v' = 0)$ and $(X^2\Sigma_g^+, v_i'' = 0)$ states, respectively. The statistical weights, $\xi(N'')$, of the total nuclear spin of $N_2^+(X^2\Sigma_g^+)$ are 6 and 3 for the even- and odd-numbered N'' levels, respectively. The transition frequency at the band origin is $\nu_{00} = 25\,566.1$ cm^{-1} (391.14 nm). In Fig. 2(a) the

calculated spectrum at $T = 300$ K is indicated by the solid line. Experimental data points appear to gather around this curve. By simulation, the rotational temperature is estimated to range from 250 to 300 K. This suggests that no marked rotational excitation occurs in $N_2^+(X^2\Sigma_g^+, v_i'' = 0)$ from N_2 . In this connection, a change in the rotational quantum numbers is found to be no more than two for direct ionization of $N_2(X^1\Sigma_g^+, v = 0) \rightarrow N_2^+(X^2\Sigma_g^+, v = 0)$ with a 21.218 eV photon (Baltzer *et al.*, 1992). The smaller signal-to-background ratio in Fig. 2(b) prevents us from estimating the rotational temperature of $N_2^+(X^2\Sigma_g^+)$ from N_2O . Berkowitz & Eland (1977) have assumed that $N_2^+(X^2\Sigma_g^+)$ is produced by direct ionization or autoionization to $N_2O^+(B^2\Pi)$, which is subsequently predissociated by a repulsive state. If this is the case, the degree of rotational excitation of N_2^+ may strongly depend on the time required for conversion of $N_2O^+(B^2\Pi)$ to the repulsive state and the potential energy curves of these states with respect to the bond angle.

In summary, we have developed a synchrotron radiation–laser combination system to perform laser-induced fluorescence excitation spectroscopy of N_2^+ ions produced by VUV excitation of N_2 and N_2O . In the near future, similar pump-probe techniques will be widely available in the study of the photodissociation dynamics of gaseous molecules in the VUV and soft X-ray regions.

We gratefully thank Professor Nobuhiko Sarukura and Dr Yasumasa Hikosaka of the Institute for Molecular Science (IMS) for fruitful discussions and their valuable help in developing the present laser system. Our thanks are also due to the members of the UVSOR facility, especially to Mr Eiken Nakamura, for their help during the course of the experiments. This work was financially supported by national funds appropriated for special research projects of IMS.

References

- Baltzer, P., Karlsson, L. & Wannberg, B. (1992). *Phys. Rev. A*, **46**, 315–317.
- Berkowitz, J. & Eland, J. H. D. (1977). *J. Chem. Phys.* **67**, 2740–2752.
- Herzberg, G. (1966). *Molecular Spectra and Molecular Structure, I. Spectra of Diatomic Molecules*, p. 126. New York: Van Nostrand.
- Hikosaka, Y., Hattori, H., Hikida, T. & Mitsuke, K. (1997). *J. Chem. Phys.* **107**, 2950–2961.
- Ishiguro, E., Suzui, M., Yamazaki, J., Nakamura, E., Sakai, K., Matsudo, O., Mizutani, N., Fukui, K. & Watanabe, M. (1989). *Rev. Sci. Instrum.* **60**, 2105–2108.
- Mizutani, M., Tokeshi, M., Hiraya, A. & Mitsuke, K. (1997). *J. Synchrotron Rad.* **4**, 6–13.
- Nahon, L., Duffy, L., Morin, P., Combet-Farnoux, F., Tremblay, J. & Larzillière, M. (1990). *Phys. Rev. A*, **41**, 4879–4888.
- Nahon, L., Morin, P., Larzillière, M. & Nenner, I. (1992). *J. Chem. Phys.* **96**, 3628–3635.
- Nahon, L., Svensson, A. & Morin, P. (1991). *Phys. Rev. A*, **43**, 2328–2337.
- Nebel, A. & Beigang, R. (1991). *Opt. Lett.* **16**, 1729–1731.
- Shaw, D. A., Holland, D. M. P., McDonald, M. A., Hopkirk, A., Hayes, M. A. & McSweeney, S. M. (1992). *Chem. Phys.* **163**, 387–404.